Engineering of Science and Military Technologies
Volume (2) - Issue (2) - Apr 2018

ISSN: 2357- 0954
DOI: 10.21608/ejmtc.2018.3246.1076

Manufacturing of a-Si/µc-Si thin-film solar cell using PECVD and silver coating

Heba R. Abd El-Aaty[1], Ossama Tobail[2], Madiha A. Shoeib[3], Iman S. El Mahallawi[4]

[1]Department of Metallurgical Engineering, Faculty of Engineering, Cairo University, [2]Nano-Technology Centre, Cairo University, Sheikh Zayed Campus, Faculty of Engineering, Zewail City, [3]Department of Surface Treatment and Corrosion Control, Central Metallurgical Research and Development Institute CMRDI, [4]Department of Metallurgical Engineering, Faculty of Engineering, Cairo University, Egypt, Centre for Renewable Energy, The British University in Egypt

Original Article

Key words:
Amorphous/ microcrystalline thin-film silicon solar cells, PECVD, PV

Corresponding Author:
El Mahallawi, Iman, Department of Metallurgical Engineering, Faculty of Engineering, Cairo University, Egypt, **Tel:** 01006044661.
Email: ielmahallawi@bue.edu.eg.

Abstract
Thin films of mixed amorphous/microcrystalline-phases have been researched during the last decade for manufacturing silicon solar cells. In this work, the Plasma Enhanced Chemical Vapor Deposition PECVD process parameters; namely, dilution ratios and substrate temperature were controlled to build a p-i-n integrated junction at low dilution ratios with moderate substrate temperatures. In the first part of this work, an intrinsic layer was deposited on Indium Tin Oxide ITO glass by PECVD technique with different dilution ratios of silane in hydrogen to study the transition from amorphous to microcrystalline phase. Based on the results of this work, and in order to study the efficiency of the solar cell and the optical properties, the second part of the work included applying a layer of nano-silver by PVD technique at a range of temperatures up to 250ºC on one selected i-layer condition at a H2/SiH4 gas dilution ratio of 13.3 at 250ºC. The Si thin film was evaluated by field emission scanning electron microscopy, X-ray diffraction and atomic force microscopy. The performance of the a-Si:H/µc-Si:H solar cell was evaluated by current-voltage measurements and optical absorption. An efficiency of 5.98% is reported for this condition with an optical absorbance of 74% at 300nm wavelength (ultraviolet and near visible region).

I. INTRODUCTION

The silicon PV bulk and thin-film solar cells are amongst the most developed and widely known technologies integrating renewable sources[1, 2]. The abundance of Si on the earth crust and its ease to deposit on various types of substrates at low fabrication temperature (T<400°C) promises continuous use of Si solar cells[3, 4]. The first Si PV thin- film solar cell was made in 1974 by David Carlson. A schematic of thin- film solar cell is shown in Fig. 1[5, 6].

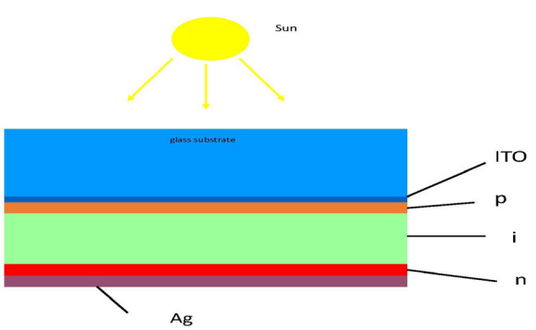

Fig. 1: Schematic of thin film solar cell

The main limitation of using a-Si is related to its light induced degradation ("Staebler-Wronski" effect) which causes non-stabilized efficiencies, it was found in 1977 that the dark conductivity and photoconductivity of glow-discharge deposited amorphous silicon can be reduced significantly by prolonged illumination with intense light. During the deposition process of amorphous silicon on a substrate the silicon atoms interact with the hydrogen atoms, the resulted layer is disordered (not a perfect crystal) and results low deposition power. All bonding atoms have different direction bonding angles and lengths due to this disorder. Sometimes a silicon atom sits where it only shares three valence electrons instead of the four which it can support. The final valence electron acts as a defect state which prefers holes for recombination. This defect is localized around an atom with one less covalent bond than expected, it is called a “dangling bond”. While hydrogenated microcrystalline silicon (µc-Si:H) does not degrade by time[7-14].

Previous studies have highlighted the effect of deposition parameters of PECVD process on the performance of the a-Si:H thin-film solar cells[15-18]. It has been shown[14, 19] that light induced degradation is enhanced for a-Si:H thin-

film solar cell, by controlling the PECVD manufacturing parameters; namely, dilution ratios, pressure and substrate temperature (TS). However, it was shown that although the degradation was enhanced at low pressure and high TS, the deposition parameters at high TS lead to increase in the defects density of the solar cell resulting from loss of hydrogen[20-22]. To avoid problems associated with high TS, some researchers adopted annealing as a route for forming polycrystalline thin-film structures[23-26]. Generally, annealing has shown to induce crystallinity. Previous work[24] has shown that the lifetime of solar cells increases at annealing temperature range 450-550K, while at greater than 550K, the lifetime suddenly decreases.

It is recognized[27-32] that PECVD process parameters can be controlled to result structures with mixed phases of a-Si:H/µc-Si:H through gas dilution and the same structure control could be achieved via annealing. In both cases, the previous work has shown that the resultant structures of the junction were controlled and accordingly its efficiency was affected. Moreover, the light absorption of the thin-film solar cells could be enhanced through control of film thickness[27], where the maximum absorption was achieved for 2nm thickness, and the minimum absorption was achieved for 11nm thickness at 630nm wavelength.

The final efficiency of a thin-film p-i-n junction and its structure are a net result of PECVD process parameters and light entrapment techniques. The manufacturing parameters include gas dilution ratio, substrate temperature and pressure and power parameters. The literature review has shown wide interest among researchers in studying the power and pressure parameters, dilution ratios and substrate temperatures. Although the bad effect of high dilution ratios on light degradation is reported, up to our knowledge, no work has investigated the solar cell properties for low dilution ratios at different substrate temperatures. Moreover, the state-of-art techniques for adopting gas dilution for obtaining the mixed i-layer structure depend on the deposition temperature, while the final metallization stages are also conducted at a variety of temperatures. The final metallisation temperatures used should not harm the previous adopted temperatures for i-layer deposition. Therefore, the aim of this work is to investigate the combined effect of the gas dilution ratio rH and the substrate temperature TS manufacturing parameters for the i-layer on the transition from amorphous to microcrystalline structure and to correlate the microstructure characteristics with the conversion efficiency and the optical properties of a-Si:H/µc-Si:H thin-film solar cell.

2. EXPERIMENTAL WORK

2.1 Sample preparation

The substrate was prepared before the deposition process, to assure its surface cleanness, by cleaning the substrate surface using methanol for degreasing followed by drying with dustless paper. When the ITO glass substrate became ready, it was installed in the substrate holder and introduced into the chamber.

The PECVD unit used in this work is Elettrorava SPA Torino Italy Model PECVD. It is a clean room compatible and versatile state-of-the art system for the deposition of thin-film devices based on silicon alloy which is designed to be ultra-compact. The process gas manifold consists of eight gas lines (CH4, C2H2, SiH4, O2, PH3, B2H6, H2 , Ar), where Ar from cylinders stored outside the lab (for safety reasons) reaches the vacuum chamber into tubes controlled by valves with pressure, this chamber is double walled and cooled by water continuously controlled by water in valve. The substrate heater is a flange with heater on top chamber; it stays in a separate vacuum chamber with adequate thermal isolation. The maximum heater temperature can reach 1000°C. The heater cavity is pumped independently using a combination of turbomolecular pump ETC80I/S backed by a fore pump, 15m3/hr capacity.

2.2. The deposition of i-layer for optimizing PECVD parameters for obtaining microcrystalline structure.

For building this layer, two gases are fed into the chamber, silane (SiH4) diluted by hydrogen gas H2. The deposition process began with pressing the silane gas in the gas line reaching the device chamber. This was followed by pressing hydrogen gas H2, by keeping the operation parameters constant, as follows: the power at 10W, the electrode distance 25cm, the plasma frequency 13.56MHz, the deposition time 15minutes, the gas pressure 1mbar, the substrate temperature was varied in series; 35, 150, 250 and 300°C. In the case of i-layer, two gases only were fed (silane gas SiH4 diluted by hydrogen gas H2) with constant hydrogen flow rate of 200sccm and silane flow rate varied in series; 40, 30, 20, 15, 10, 7sccm (meaning dilution ratios (rH) 5, 6.7, 10, 13.3, 20, 28.7).

The operation parameters of i -layers are summarized in Table 1 and Table 2. The deposition time was 15min, the gas pressure was kept at 1mbar. The plasma power used was 15W and it was kept fixed for all specimens during all the experiments.

Table 1: The operation parameters of i-layer with dilution ratio series

Specimens no.	Silan flow rate [Sccm]	Hydrogen flow rate [Sccm]	Dilution ratio H2/ SiH4	Time [min]	Substrate Temperature [°C]
1	40	200	5	15	250
2	30	200	6.7	15	250
3	20	200	10	15	250
4	15	200	13.3	15	250
5	10	200	20	15	250
6	7	200	28.7	15	250

Table 2: The parameters of i-layer with substrate temperature series

Specimens no.	Silan flow rate [Sccm]	Hydrogen flow rate [Sccm]	Dilution ratio H2/ SiH4	Time [min]	Substrate Temperature [°C]
1	15	200	13.3	15	35
2	15	200	13.3	15	150
3	15	200	13.3	15	250
4	15	200	13.3	15	300

2.3 Building the p-i-n junction

The p-i-n junctions were prepared as follows:

2.3.1 The deposition of p-layer.

The p-layer is deposited in this work by feeding three gases as follows: silane gas (SiH4) diluted by hydrogen gas (H2) and doped by diborane gas (B2H6). The deposition process began with pressing the silane gas in the gas line reaching the device chamber. This was followed by pressing hydrogen gas H2, followed by the diborane gas B2H6 to build the p-layer on the glass substrate. The operation parameters were kept constant as follows: the power at 10W, the electrode distance 25cm, the plasma frequency 13.56MHz, the vacuum pressure 1x10-4 mbar, the gas pressure 1mbar, the Silane flow rate SiH4 13sccm, the hydrogen flow rate H2 200sccm, the diborane flow rate B2H6 3sccm, the deposition time 10min; and the substrate temperature (TS) 250°C.

2.3.2 The deposition of i-layer.

The device chamber was prepared to build i-layer on the p-layer by keeping the operation parameters constant. The same procedures described in 2.2 were followed at this stage, but the optimum parameters (based on the results obtained in this work) were selected which was: silane flow rate; 15sccm (meaning dilution ratio (rH= 13.3). The deposition time was 15min, the gas pressure was kept at 1mbar. The plasma power used was 10W and it was kept fixed for all specimens during all the experiments.

2.3.3 The deposition of n-layer.

The n-layer is the last layer of p-i-n structure. In this layer, three gases were fed: (silane gas SiH4) diluted by hydrogen gas H2 and doped by Phosphine PH3. It was built on the i-layer by keeping the operation parameters constant as follows: the power at 10W, the electrode distance at 25cm, the plasma frequency 13.56MHz, the vacuum pressure 1x10-4mbar, the gas pressure 1mbar, the silan flow rate (SiH4) 13sccm, the hydrogen flow rate (H2) 200sccm, the phosphine flow rate (PH3) 5sccm, the deposition time 10min, and the substrate temperature (TS) at 250°C.

The deposition time was 10min for both p and n layers and 15min for the i-layer, the gas pressure was kept at 1mbar. The plasma power used was 15W, and it was kept fixed for all specimens during all the experiments.

2.4 The deposition of nano-silver layer.

The PVD unit used for depositing the nano-silver layer is a Plasma Sputtering Coater, USA MTI Company model VTC-16-3H. One condition of the p-i-n junction with i-layer substrate temperature of 250°C and rH of 13.3 was selected for silver deposition. The deposition conditions for depositing the nano-silver layer on the silicon thin

film are as follows: vacuum pressure 43 pa, Ar flow rate 45sccm, three minutes process time, 9mA current, 1500W deposition power and substrate temperature in the range of 35-250°C. These conditions were selected by the authors in view of the experimental work showing that they lead to the formation of nano-size silver particles, and they are not reported in this work, as the focus of this work is the PECVD deposition conditions and the silver layer is only added for following absorbance and IV efficiency measurements. Before each deposition process the target surface and the device chamber were cleaned by methanol to remove any oxides.

The prepared i-layer specimens with different conditions were characterized by Field Emission Scanning Electron Microscopy (FESEM), Atomic Force Microscopy (AFM) and X-ray Diffraction (XRD). After the integration of the p-i-n junction and applying the nano-silver layer at different substrate temperatures, the performance of the thin-film solar cell was evaluated using current -voltage measurements (I-V) and optical absorption.

2.5. Morphology characterization

2.5.1 Field emission scanning electron microscope FESEM.

Field emission scanning electron microscopy (FESEM) provides topographical and elemental information at magnifications of 10x to 300,000x with virtually unlimited depth of field. Compared with convention scanning electron microscopy (SEM), field emission SEM (FESEM) produces clearer, less electrostatically distorted images with spatial resolution down to 1.5 nanometers, three to six times better. In this work, QUANTA FEG 250 device model was used. FESEM was performed on the ITO glass substrate and selected i-layer deposited specimens resulting from PECVD.

2.5.2 Atomic force microscope AFM.

AFM was used to study the surface roughness. AFM study was performed on the ITO glass substrate and i-layer deposited specimens for different conditions produced from PECVD process. In this work, an AFM Solver Next SPM controller NT-MDT P9 XPM Systems Digital Control Platform is used.

2.5.3 X-Ray diffraction.

XRD was used to detect the transition from amorphous to crystalline phases of the Si:H thin-film i-layer deposited by PECVD technique at different dilution ratios and at different substrate temperatures. BRUKER AXS D8Advance, Germany production, X-Ray Diffractometer with a copper target (Cu k α = 1.54060) and nickel filter is used in this work. The testing conditions were as follows: 0.02 deg. step size and 0.4 sec. time per step.

2.6 Evaluation of the performance of the solar cell

2.6.1 Current -voltage measurements (I-V).

A PV system analyzer LANGLOIS model VA1011 was used in this work for current-voltage measurements. The cell was connected to the PV system analyzer, which is equipped with an irradiance sensor and thermometer to detect the light intensity and the outdoor temperature during the test. The current-voltage measurement (I-V data) was recorded and used to determine the cell efficiency, fill factor, open circuit voltage, short circuit current, maximum power, maximum voltage and maximum current.

2.6.2 Optical absorption.

The optical properties of the a-Si/µc-Si thin-film cell was studied by measuring its optical absorption using spectrophotometer V-770 Jasco with halogen lamp 190 to 350nm, photomultiplier tube detector, in the wavelength range 300 to 2500nm. The light incident on the photomultiplier tube is converted into an electrical signal and, after being subjected to synchronous rectification; it is converted to a digital signal. The signal is processed by the computer showing on the monitor a diagram of the relation between absorption and the selected wavelength.

3. RESULTS AND DISCUSSION

3.1 Morphology of i-layer deposited specimens.

Fig. 2 shows the FESEM surface images of specimen no. 4 and 6 in Table 1 (i-layers deposited on ITO glass substrate specimens produced using PECVD process). The resulted thickness of the thin film under these conditions are the same value 450nm, it is measured by cross section view method

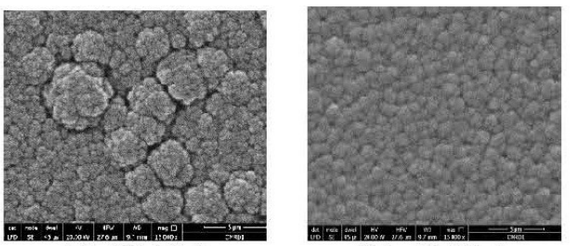

(a) rH 13.3 (b) rH 28.6

Fig. 2: FESEM images for Si thin-film at TS 250°C

It is shown from Figs. 2a and 2b of the surface image of the i-layer deposited on ITO glass substrate specimens at different dilution ratios (rH) and at TS=250^{o}C, that the FESEM surface image of the i-layer deposited on ITO glass substrate at (rH13.3) shows the start of the transition, whilst at (rH28.6) complete transition from amorphous to microcrystalline structures is achieved. Fig. 2a illustrates that the surface is combined of microcrystalline and amorphous phases, where the microcrystalline grains collect together to form grains with average grain size of 390nm with rounding of the pyramidal peaks and ridges and sharpening of the valleys. It is also shown that the phases are not homogenously distributed on the surface. Fig. 2b shows a completely microcrystalline phase. The microcrystalline grains are seen as isolated roughly circular objects. Many grains have already collided and formed an irregularly connected network of grains of average grain

size 395nm. The non-classical theory of crystallization of thin films explains crystal growth by building block of nanoparticles, rather than forming clusters from atoms, ions or molecules[33]. This theory is based on the generation of charged nanoparticles which become a dominant flux for the growth of thin films and nanostructures[33].When these charged particles are dominant over neutral particles, better quality thin films free from voids are obtained. The size of these charged nanoparticles has been shown[33] to depend on flow rate of reactant gases, reactor pressure and inert gas flow rate. The number density of these particles increases with the reactor temperature. The formation of nanocrystalline or microcrystalline grains embedded in an amorphous matrix has been explained in view of the non-classical crystallization theory to result from nanocrystals forming in the electrically charged gas phase nuclei[33].

Fig. 3 shows the AFM images of specimen no. 1, 2, 3, 4, 5 and 6 in Table 1. The scanned area was 5x5µm. The scanned operation was at contact tip mode. The values of their surface roughness were measured directly from the device screen as 6, 8.8, 11, 22.5,50 and 50nm, respectively.

(a) rH 5 (b) rH 6.7 (c) rH10 (d)rH13.3 (e)rH20 (f)rH 28.7

Fig. 3: AFM images of ITO substrate and dilution series at TS 250°C

The morphology of the i-layer surface is affected by changing the gas dilution ratio. Fig. 3a shows the i-layer deposited on ITO glass at rH=5, where the surface appears to consist of smooth amorphous Si. The structure undergoes a transition from a rather smooth amorphous surface to amorphous structures with only a few isolated grains, at rH values of 6.7, 10, 13.3; Fig. 3b, Fig. 3c, and Fig. 3d; respectively. When the rH value was 20 (Fig. 3e), the surface consisted of a rough µc–Si:H surface composed of grains (aggregates) with a typical cauliflower structure. At rH=20, the surface roughness value was calculated as 50nm. At higher values of rH (rH=28.7) the nucleation density increases and much smaller grains were formed with surface roughness value of 50nm. Roughening transition of the interface is explained[33] to result from differences between edge energy and surface energy induced by temperature. The roughening of the interface causes the barrier for 2D nucleation to become zero, which means that the interface changes from smooth to rough and has no barrier for atomic attachment[33]. This results from the hydrogen induced rise in the Si atom mobility which has an inverse relationship with the nucleation density[34]. For deposition of silicon films by PECVD, silane SiH4 is used as a source of silicon and hydrogen is used to control the decomposition of the reaction. The final density of grains and grain size is shown[33] to be a result of deposition and etching of silicon, which occur simultaneously, and which depends on the silicon precipitated in the gas phase. Combining the results obtained from FESEM and AFM, it can be concluded that the surface roughness is affected by grain size as well as crystallinity. The roughness increases with crystallinity and decreases with grain size. This will affect the light absorption, as light absorption is enhanced by surface roughness[34]. It is worth mentioning that both Fig. 3a and Fig. 3f show the same morphology, Fig. 3a at rH 5 is a fully amorphous Si phase where Fig. 3f at rH 28.7 is almost fully microcrystalline Si phase. The difference between the two conditions will be further evaluated by X-ray diffraction.

Fig. 4 shows the FESEM surface images of specimen no. 1 and 3 in Table 2 (i-layers deposited on ITO glass substrate specimens produced using PECVD process). The resulted thickness of the thin film under these conditions are 220nm and 450nm, it is measured by cross section view method.

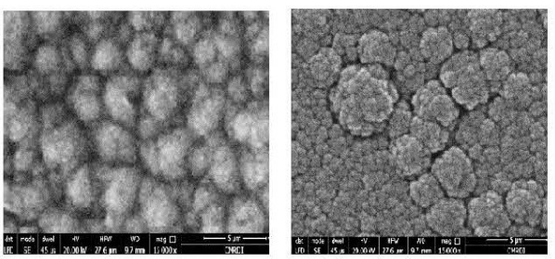

(a) 35°C (b) 250°C

Fig. 4: FESEM images for Si thin film with different substrate temperatures at rH 13.3

Fig. 4a shows the surface image of i-layer at TS 35°C. The figure illustrates a-Si:H phase without any crystalline Si growth. Fig. 4b describes the same deposition conditions as Fig. 4a except that being deposited at TS 250°C. It is shown that the above mentioned conditions (in table 2) led to an increased thin-film thickness from 220nm to 450nm suggesting that the deposition rate increases when TS increases. This is explained by the more physisorpted reactive radicals that would transform to chemisorpted, when TS increases as the condensation coefficient of the reactive radicals would be improved. Since the deposition rate is controlled by the condensation coefficient of the film precursors on the growing surface[27], the promotion of the deposition rate is associated with the increase in the substrate temperature. Also, during the deposition, part of the chemisorpted H atoms produced by silane dissociation would balance the dangling bonds on the growing surface and would hinder the adsorption of the film precursors[28]. The substrate deposition temperature was shown to have a direct impact on the mobility of the precursors on the surface promoting their diffusion, desorption and chemical reactions, thus influencing the structure and content of deposited thin film[21].

The microstructural features depicted in Fig. 4 illustrates rounding of the pyramidal peaks and ridges and a sharpening of the valleys with average grain size of 350 nm. The surface is combined of microcrystalline Si grains growing among amorphous Si tissues; where the microcrystalline grains begin to collect together. The a-Si:H/µ-Si:H mixed phase film results from the increase in TS and the crystalline volume fraction increases accordingly. The results can be explained in view of the self-diffusion activity of Si atoms and the deposition rate[30]. The nucleation density increases when the conditions are shifted to the µ-Si:H growth. The reason for the appearance of isolated µc–Si:H grains on the surface of the samples with TS 250°C is attributed to higher thickness of the deposited films[31, 32].

Fig. 5 shows the AFM images of specimen no. 1, 2, 3 and 4 in Table 2. The scanned area was 5x5µm. The scanned operation was at contact tip mode. The values of their surface roughness are calculated as 8.9, 32.8, 22.5 and 17.2nm, respectively.

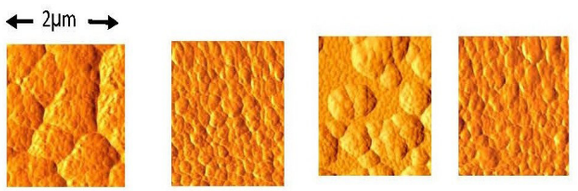

(a) 35°C (b) 150°C (c) 250°C (d) 300°C

Fig. 5: Surface topography of the samples of the substrate temperature series by AFM microscope at rH 13.3

Fig. 5a shows that at dilution ratio (rH13.3) and TS 35°C, the study obtained fully a–Si:H sample with a higher band gap[33] which hinders the absorption of the incident sun light, since if the photon energy is lower than the band gap energy it cannot be absorbed. If the photon energy is higher than band gap energy it will be reduced to the band gap energy by thermalization of the photogenerated carriers[33]. By increasing TS to 150°C (Fig. 5b), the crystalline volume fraction (crystallinity) would increase due to the enhanced self-diffusion of Si leading to increasing the surface roughness values. However, when the substrate temperature is further increased (TS ≥250°C) (Fig. 5c, Fig. 5d)) though several grain clusters are seen to cover the growth surface, it seems that many of them had insufficient time to grow to crystals, which resulted reduced crystallinity and led to mixed amorphous and microcrystalline structure. The effect of increased deposition temperatures of the substrate on the decrease of the crystalline orientation degree led to a decrease in the surface roughness values. It has been reported that the defect density decreases with increasing the substrate temperature[34-39].

In this work, the transition between a-Si:H to µc-Si:H by using PECVD and different gas dilution ratios and different substrate temperatures was achieved at rH 13.3 and 250°C. Previous trials by Xiaonan Wang *et al*[23] included depositing a-Si thin films on glass substrates by PECVD process, and annealing in high-purity argon gas (99.999%) for 2 h at various temperatures of 400 ºC, 500 ºC, 600 °C, 650 °C, 700 °C to achieve the transition between a-Si:H to µc-Si:H at 650 ºC annealing temperature[23]. Whereas, Jong-Bae Park *et al*[26] used plasma electron annealing process for achieving the recrystallization of a-Si thin films. The process was conducted in a vacuum chamber having a base pressure of 2.6 × 10−4 Pa and filled with helium to a working pressure of 0.67 Pa, with Radio frequency (RF) power of 200W at 12.56 MHz. The annealing temperatures were 536°C, 718°C and 863°C for 60 sec, decreased gradually to 100°C for 160 sec. They achieved recrystallization where the amorphous Si films were almost completely changed to polycrystalline Si films without damaging the surface[26].

3.2 X-Ray diffraction of the i-layer deposited specimens.

In this section, the effect of the gas dilution ratio of PECVD process on the crystallinity of Si:H thin-film is discussed in view of X-Ray Diffraction. Fig. 6 shows the XRD patterns of all the produced specimens described in Table 1, from which it is shown that the resulting phase is polycrystalline silicon. Fig. 6 illustrates that the maximum intensity appears for the saline dilution ratio (rH= 28.6), and the minimum intensity appears for the saline dilution ratio (rH = 5). It is also shown that a slight peak appeared at the diffraction angle 2Θ = 28° for dilution ratio 13.3 at (111) crystallographic Si plane, which indicates a clear transition to the crystalline structure c-Si:H4. These results comply with the FESEM and AFM results reported earlier in Fig. 3 and Fig. 4. The samples with rH ≥20 indicate some degree of crystallinity with a slightly preferential peak of the (111) crystallographic Si plane and much weaker response for (220) and (311) Si planes. The XRD patterns of the samples with rH=28.6 show larger peaks at (111), (220) and (311) compared with the peaks at rH 20.

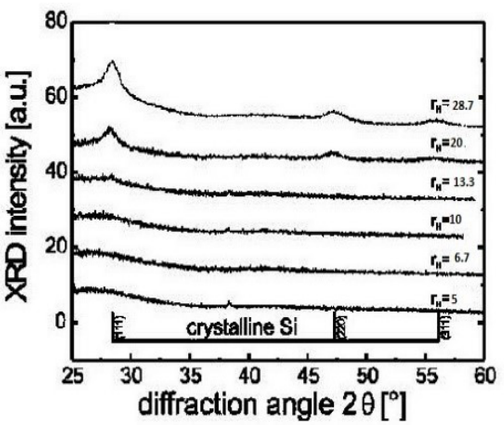

Fig. 6: XRD patterns of the samples of the dilution series at TS 250°C

The results of the XRD patterns of the samples of the dilution series show that the increase in the hydrogen dilution ratio (in the plasma during the film deposition process) increases the sharpness of the (111) plane which indicates the presence of crystalline structure and substantial preference of nucleation of (111) grains over (220) at rH = 20[21]. It has been reported that increasing the hydrogen dilution ratio further decreases the (111) and (220) nucleation density. This results from the hydrogen induced rise in the Si atom mobility, which has an inverse relationship with the nucleation density[22].

Accordingly, it can be stated that an XRD peak appears at (111) Si crystallographic plane near the a-Si:H to µc-Si:H transition region at (rH = 13.3), which subsequently increases with increasing hydrogen dilution ratio. Excess atomic hydrogen flux onto the film surface compared with silane flow rate increased the mobility of the precursors, which reduced the nucleation density. However, the reduction of the (220) nucleation density was offset by the high density of SiH3 precursors produced during the Plasma running. This implied that the crystallinity increased at rH >13.3.

The slight appearance of crystallinity, at hydrogen dilution ratios of 13.3, results from the depletion of SiH4 molecules in the plasma. This occurs due to the low silane flow rate (15sccm). Thus, the reactive species forming within the plasma could not react with other SiH4 molecules or radicals. As a result, during the deposition process, these reactive species were automatically incorporated in the film. Additionally, the higher atomic hydrogen flux density on the film surface not only etched the film but also reacted with the surface atoms. This increased the number or density of vacant sites that were included in the resultant film due to the lack of SiH3 precursors available to take up these sites. The aforementioned phenomena led to an increase in the crystallinity of the film[36, 37].

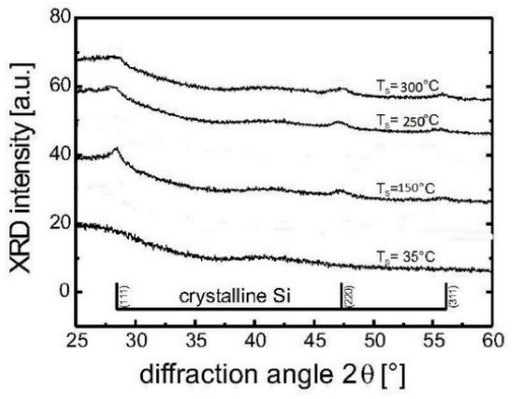

Fig. 7: XRD patterns of the samples of the substrate temperature series at rH 13.3

Fig. 7 shows the XRD patterns of all the produced specimens described in Table 2. The figure indicates that at TS 35°C the deposited i-layer is pure amorphous SiH4 whereas no peaks appear in the graph. With increasing the TS to 150°C the presence of (111) crystallographic plane of the Si grains is confirmed. When the substrate temperature is increased to 250°C and 300°C, the presence of (111) crystallographic Si planes diminishes. This is interpreted by the effect of deposition temperature on the diffusion of the deposited atoms. When the substrate temperature increases, both the self-diffusion activity of Si atoms and the deposition rate increase.

By correlating the data resulting from FESEM, it is shown that the film thickness increases from 220nm to 450nm with TS increasing from 35°C to 250°C. Conditions enhancing self-diffusion lead to the improvement of the crystallinity. Higher self-diffusion activity of Si atoms are achieved with increasing substrate temperature (TS ≤ 150°C) compared to sufficiently low substrate temperatures. The transformation to crystalline grains occurs due to the enhanced self-diffusion of Si. However, when TS increases to 250°C, the increased presence of clusters covering the growth surface, results insufficient crystallization time to grow the crystal nuclei, leaving the amorphous structures to exist, resulting decrease of the crystallinity. As TS increases to 250°C, the activity of the atoms would be increased significantly. The transition from amorphous phase to crystalline phase occurs (at TS =250°C), as the unstable atoms have enough energy to move to lower energy positions. At TS < 250°C a number of strained and broken bonds in amorphous silicon lead to low surface mobility of the reactive radicals at the growth surface. While at substrate temperature > 250°C loss of hydrogen perfusion in the deposited film leads to increase in the defect density. In this work, the transition between a-Si:H to µc-Si:H by using PECVD and different substrate temperatures was achieved at TS 250°C. Similar findings were reported before[39-41].

Based on this part of the work, the p-i-n junction with i-layer substrate temperature of 250ºC and rH 13.3 was selected for further silver deposition, as the aim of this work is to study the mixed amorphous- microcrystalline structures.

3.3 Current-Voltage measurements (I-V)

This section describes the performance of the p-i-n junction deposited by PECVD process with the nano-silver layer. The specimen no. 3 in Table 2 was selected for further silver deposition by PVD process. PVD parameters were deposition time 3 minutes, 9mA current, 1500Wdeposition power, at 200 and 250°C substrate temperatures.

Figs. 8 and 9 show the current-voltage relation of µc-Si:H solar cell under the previous conditions, the open circuit voltage records 0.47V, short circuit current 10 mA, maximum power 2.4 mW, the fill factor of 48.4% with

efficiency 5.89% was obtained at substrate temperature 250ºC. The open circuit voltage records 0.47V, short circuit current 10 mA, maximum power 2.4 mW, the fill factor of 48.4% with efficiency 5.98% was obtained at substrate temperature 200ºC. S. Steffensa[42] have attributed the role of temperature to the enhanced current collection attributed to the abrasion etch light trapping structures scattering the incoming photons, hence lengthening their path way in the photovoltaic material and increasing the probability of absorption.

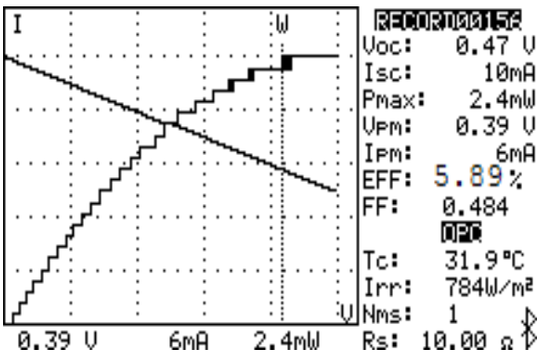

Fig. 8: I-V Characteristics of µc-Si:H solar cell with nano-silver film by PVD process at 250ºC

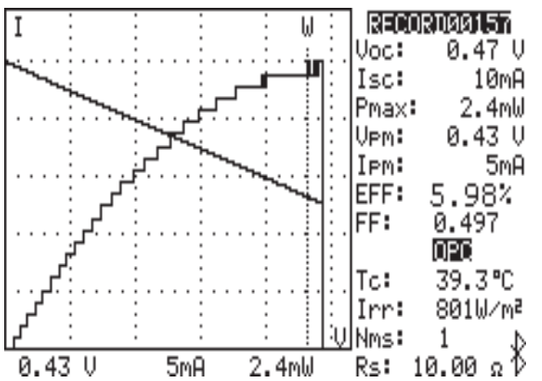

Fig. 9: I-V Characteristics of µc-Si:H solar cell with nano-silver film by PVD process at 200ºC

3.4 Optical absorption

Fig. 10 shows the absorption (with wavelengths varying from 300nm to 2500nm) of the µc-Si:H solar cell deposited by PECVD process with a nano-silver layer by PVD at the same deposition conditions at sec. 3.3, with substrate temperature 250ºC. The maximum absorbance percentage recorded was 70% with wavelengths 300nm (near ultraviolet), then suddenly dropped to about 17% with wavelength 500nm (violet), and the drop continued to drop to 7% at wavelength 900nm (near infrared). This is related to the surface plasmon resonance SPR property of spherical silver nanoparticles (the conduction electrons on the nano-silver surface undergo collective oscillation when excited by light at these wavelengths).

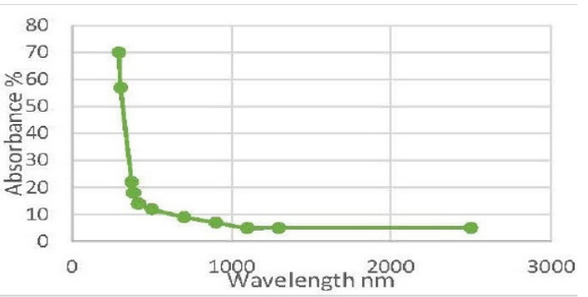

Fig.10: Absorbance of µc-Si:H solar cell with a nano-silver layer by PVD process at substrate temperature 250ºC

Peak wavelength can be tuned from 400 nm (violet light) to 530 nm (green light) by changing the particle size and the local refractive index near the particle surface[35]. Similar findings were reported before[43, 44], where the maximum absorbance was 65% reported at 300nm wavelength. The nano-silver layer is shown to act as a good absorption and light trapping of sun light. In combination with the light trapping effect of the nano-silver layer in a medium of silicon with a high index of refraction, it increases the current generated in thin-film silicon solar cells[35].

3.5 Effect of silver deposition substrate temperature

Fig. 11 shows the absorption (with wavelengths varying from 300nm to 2500nm) of the p-i-n junction deposited by PECVD process, with the nano-silver layer deposited by PVD process at different substrate temperatures. The deposition conditions are given in Table 3.

Table 3: The deposition parameters of nano silver by PVD

Time min	Current mA	Deposition power watt	Substrate temperature ºC	Size of nano silver particles, nm, measured by FESEM
3	9	1500	30	50
3	9	1500	100	55
3	9	1500	150	55
3	9	1500	200	66
3	9	1500	250	79

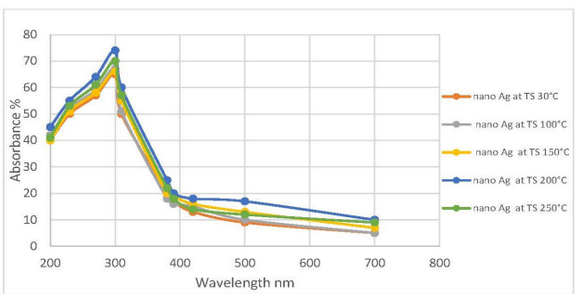

Fig. 11: Absorbance of µc-Si:H solar cell with a nano-silver layer by PVD process deposited at 30, 100, 150, 200, and 250°C substrate temperatures TS

The absorbance percentage values ranged from 50 to 70% with wavelengths varying from 300nm to 350nm (near ultraviolet), then suddenly dropped to about 20% with wavelength 400nm (violet), and the drop continued to 7% at wavelength 900nm (near infrared). This is related to the surface plasmon resonance SPR property of spherical silver nanoparticles (the conduction electrons on the nano-silver surface undergo collective oscillation when excited by light at these wavelengths). Peak wavelength can be tuned from 400 nm (violet light) to 530 nm (green light) by changing the particle size and the local refractive index near the particle surface [34].

In this work, light trapping was achieved by applying a nano-silver layer over the mixed phase a-Si:H/µc-Si:H solar cell using PVD with different substrate temperatures. The maximum absorbance of 74% was obtained for the Si thin-film solar cell with nano-silver layer deposited by PVD process at substrate temperature 200°C, with 88nm surface roughness, at 300nm wavelength (ultraviolet and near visible region), and dropped suddenly to 17% at 500nm wavelength (visible and near infrared region). Similar findings were reported before [43, 44], where the maximum absorbance was 65% reported at 300nm wavelength. The nano-silver layer is shown to act as a good absorption and light trapping of sun light. In combination with the light trapping effect of the nano-silver layer in a medium of silicon with a high index of refraction, it increases the current generated in thin-film silicon solar cells [34].
The comparison between our results and the survey results are summarized in Table 4.

Table 4: Comparison between previous results and results obtained in this work

The previous research results	Our research results
1- Xiaonan Wang *et al* 2016[23] deposited a-Si thin films on glass substrates by PECVD process, and annealing in high-purity argon gas (99.999%) for 2 h at various temperatures of 400 ºC, 500 ºC, 600 °C, 650 °C, 700 °C to achieve the transition between a-Si:H to µc-Si:H at 650 ºC annealing temperature[23]. 2- Jong-Bae Park *et al* 2017[26] used plasma electron annealing process for achieving the recrystallization of a-Si thin films. The process was conducted in a vacuum chamber having a base pressure of 2.6 × 10−4 Pa, and filled with helium to a working pressure of 0.67 Pa, with Radio frequency (RF) power of 200W at 12.56 MHz. The annealing temperatures were 536°C, 718°C and 863°C for 60 sec, decreased gradually to 100°C for 160 sec[26].	We deposited an intrinsic layer (Si:H) on Indium Tin Oxide ITO glass by PECVD technique with the substrate temperature varied in series; 35, 150, 250 and 300°C, and with dilution ratios (rH) 5, 6.7, 10, 13.3, 20, 28.7). The transition from amorphous to microcrystalline phase was achieved at TS 250°C and dilution ratio (rH) 13.3.
S. Steffensa *et al* 2013[42] deposited p-i-n structure using different deposition processes. They found that rapid thermal annealing of 1050ºC Plasma Enhanced CVD on rough substrates resulted the maximum efficiency of 6.7%, Electron Beam Evaporation on smooth substrates resulted 5.29%, Plasma Enhanced CVD on smooth substrates resulted 5.05% and laser annealed at 430ºC PECVD sample on a smooth glass substrate resulted 5.14%.	For condition number 3 in Table 2, after depositing nano-silver layer at 200°C and 250°C, the efficiencies were 5.98% and 5.89%, respectively.
Y. Battie 2011[43] and N. Ahmad 2012 [44] achieved 65% maximum absorbance.	For condition number 3 in Table 2, after depositing nano-silver layer at 200°C, the maximum absorbance achieved is 70%.

4. CONCLUSIONS

Based on this work, it was proved that amorphous to microcrystalline Si transition is achieved at rH 13.3 and substrate temperature 250°C. The efficiency achieved for these conditions was 5.89% verified for mixed phase a-Si:H/µSi:H solar cell with Ag thin film deposited by PVD process at temperature 250°C. The optical absorbance achieved was 70% for mixed phase a-Si:H/µSi:H solar cell with Ag thin film deposited by PVD process at temperature 250°C, at 300nm wavelength and dropped to 17% at higher wavelength above 500nm.
It is also proven that the substrate temperature of the silver deposition affects the structure and morphology of the silver layer. The maximum efficiency achieved in this work of 5.98% was verified for a mixed phase a-Si:H/µSi:H solar cell with nano-Ag layer deposited by PVD process at substrate temperature 200°C. The maximum absorbance achieved in this work of 74% was obtained for

mixed phase a-Si:H/μSi:H solar cell with nano-Ag layer by PVD process at substrate temperature 200°C, at 300nm wavelength (ultraviolet and near visible region), and dropped suddenly to 17% at 500nm wavelength (visible and near infrared region).

ACKNOWLEDGMENT

The Authors wish to thank the Science and Technology Center of Excellence STCE, the Central Metallurgical Research and Development Institute CMRDI and the Renewable Energy Laboratory at the British University in Egypt, for allowing their facilities to complete this work.

REFERENCES

[1] D. Ahuja, M. Tatsutani, Sustainable energy for developing countries, SAPIENS 2(1) (2009) pp1-16.
[2] M. Zeman, Thin-Film Silicon PV Technology, JEE 61(5) (2010) pp271-276.
[3] S. Pizzina, Advanced Silicon Materials for Photovoltaic Applications, Wiley (2012) pp35-40.
[4] M. Zeman, J. Krc, Optical and electrical modeling of thin-film silicon solar cells, Mat Res 23 (4) (2008) pp889-898.
[5] S. Fu, The characterization of Hydrogenated Silicon Thin-film using constant Photocurrent Method, Msc thesis National Center University Taiwan (2009) pp8-10.
[6] A. Luque, S. Hegedus, Handbook of Photovoltaic Science and Engineering, Wiley (2003) pp505-506.
[7] D. L. Staebler, C. R. Wronski, Reversible conductivity changes in discharge produced amorphous Si, APL 31 (4) (1977) pp75.
[8] P. Cuony, Optical Layers for Thin-film Silicon Solar Cells, PhD thesis Federal Institute of Technology Suisse (2011) pp4-6.
[9] T. Roschek, Microcrystalline Silicon Solar Cells Prepared by 13.56 MHz PECVD Prerequisites for High Quality Material at High Growth Rates, Research Center Jülich in the Helmholtz Association (2003) pp27-29.
[10] G. Maxwell, Characterization and Modeling OF CdCl2 Treated CdTe/CdS Thin-Film Solar Cells, PhD thesis Colorado State University Colorado (2010) pp24-31.
[11] A. Robert, Hydrogenated Amorphous Silicon. Syndicate of Cambridge University Press (1991) pp3-10.
[12] JG. Simmons, GW. Taylor, Nonequilibrium Steady-State Statistics and Associated Effects for insulators and Semiconductor Containing an Arbitrary Distribution of Traps, Phys Rev 4(2) (1971) pp502-511.
[13] A. Kolodziej, W. Staebler, effect in amorphous silicon and its alloys, Opto-Electron Rev12 (1) (2004) pp21-23.
[14] N. Wang, Improving stability of amorphous silicon using chemical annealing with helium, J Non-cryst Solids 352 (2006) pp1937-1940.
[15] S. Michard, Microcrystalline silicon absorber layers prepared at high deposition rates for thin-film tandem solar cells, Eur Phys J pv4 (45201) (2013) pp1-6.
[16] B. Modtland, Improving the light-induced degradation of hydrogenated amorphous silicon solar cells using fabrication at elevated temperatures and low pressure, PhD thesis Iowa State University USA (2013) pp13-25.
[17] T. Mates *et al*, Effect of substrate temperature and hydrogen dilution on thin silicon film system deposited at low substrate temperature, 3rd World Conference on Photovoltaic Energy Conversion Osaka Japan, 2003 pp1664.
[18]Y.H. Chen, Hydrogen dilution on an undoped silicon oxide layer and its application to amorphous silicon thin-film solar cells, Mat Sci Semicon Proc 41 (2016) pp312-316.
[19] M. Brinza, Thin film silicon n–i–p solar cells deposited by VHFPECVD at 100 1C substrate temperature, Sol Energ Mat Sol C (2008) pp1-4.
[20] K. Zellama, Systematic study of light–induced effects in hydrogenated amorphous silicon, Phys Rev B 45(23) (1992) pp13314-13322.
[21] JN. Lee, Effect of deposition temperature on the crystallization mechanism of amorphous silicon films on glass, Jpn J Apll Phys 36(11) (1997) pp6862-6867.
[22] N. Parvathala, Light induced degradation of amorphous silicon containing nanocrystalline silicon, J Apll Phys 14(047124) (2014) pp1-10.
[23] X. Wang, Microstructure evolution of amorphous silicon thin films upon annealing studied by positron annihilation, Mat Sci Semicon Proc 56 (2016) pp344-348.
[24] Y. Luo, The influence of annealing temperature upon the structure of a Si:H/c-Si thin-films, J Non-cryst Solids 471 (2017) pp379-383.
[25] P. Bellanger, Understanding phenomena of thin silicon film crystallization on aluminum substrates, Energ Procedia 84 (2015) pp156- 164.
[26] J. Bae Park, Plasma electron annealing method for recrystallization of a-Si thin films. Thin Solid Films, 622 (2017) pp111-114.
[27] D. Kar, Structural characterization of silicon thin-film super lattice grown at low temperature, Superlattice microst (2017) pp1-11.
[28] WZ. Cui, Preparation Principle Technology and Application of Thin Films, 2nd edition Metallurgical Industry Press Beijing (2003) pp151.
[29] G. Chris, Hydrogen in silicon: Fundamental properties and consequences for devices, J Vac Sci Technol A 16(3) (1998) pp1767-1769.
[30] M. Ohring, Materials Science of Thin Films, 2nd edition (2002) pp327.
[31] H. Cheng, Effects of Substrate Temperature on the Growth of Polycrystalline Si Films Deposited with SiH4+Ar, J Mater Sci Technol 25 (4) (2009) pp489-491.
[32] LQ. Song, Effect the substrate temperature on the growth and properties of boron-doped microcrystalline silicon film, Chin J Phys 15(1) (2006) pp 214-216.
[33] A. R. Jha, Solar cell technology and applications, Taylor and Francis. (2009) pp136-137.
[34] N. M. Hwang, Non-Classical Crystallization of Thin Films and Nanostructures in CVD and PVD Processes, Springer Science Business Media Dordrecht, 2016 pp1-2, 83, 94-95, 163-164, 307-308.
[35] J. Springer, Absorption loss at nanorough silver back reflector of thin-film silicon solar cells, J Apll Phys 95 (3) (2003) pp1427-1429.
[36] K. M. Azizur Rahman, Nanocrystalline Silicon Solar Cells Deposited via Pulsed PECVD at 150°C Substrate Temperature, PhD thesis (2010) pp54-56.
[37] S.N. AGBO *et al*, Deposition Pressure and Hydrogen Dilution Effects on the Spectral Response of Thin Film Nanocrysyalline Silicon Solar Cells, Journal of Ovonic Research 9(1) (2013) pp2-4.
[38] G. Ganguly *et al*, Defect formation during growth of hydrogenated amorphous silicon, Appl Phys 47 (1993) pp3661.
[39] Y. Nasuno *et al*, Passivation of oxygen–related donors in microcrystalline silicon by low temperature deposition, Appl Phys 78(16) (2001) pp2330–2332.
[40] LQ. Song, Effect the substrate temperature on the growth and properties of boron-doped microcrystalline silicon film, Chin J Phys 15(1) (2006) pp 214-216.
[41] F. Edelman, Structure of PECVD Si:H films for solar cell applications, Sol Energ Mat Sol C 77 (2003) pp131–133.
[42] S. Steffens, Defect annealing processes for polycrystalline silicon thin-film solar cells, Mater Sci Eng B 178 (2013) pp672-674.
[43] Y. Battie, Optical properties of silver nanoparticles thermally grown in a meso structured hybrid silica film, Opt Mater Express 1(5) (2011) pp1028- 1030.
[44] N. Ahmad, Ultra-Thin Metal Films for Enhanced Solar Absorption, PhD thesis, University of Bristol, UK (2012) pp2-7.